Available online at www.sciencedirect.com
ScienceDirect
Journal of Solid State Chemistry 180 (2007) 1002–1010
JOURNAL OF SOLID STATE CHEMISTRY
www.elsevier.com/locate/jssc

Cation ordering in the fluorite-like transparent conductors $In_{4+x}Sn_{3-2x}Sb_xO_{12}$ and In_6TeO_{12}

J. Choisnet[a,*], L. Bizo[a,b], M. Allix[b], M. Rosseinsky[b], B. Raveau[a]

[a]*Laboratoire CRISMAT, UMR 6508 CNRS ENSICAEN, 6 bd Maréchal Juin, 14050 Caen Cedex 4, France*
[b]*Department of Chemistry, University of Liverpool, Liverpool L697ZD, UK*

Received 10 October 2006; received in revised form 19 December 2006; accepted 24 December 2006
Available online 9 January 2007

Abstract

The cation ordering in the fluorite-like transparent conductors $In_{4+x}Sn_{3-2x}Sb_xO_{12}$ and In_6TeO_{12}, was investigated by Time of Flight Neutron Powder Diffraction and X-ray Powder Diffraction (tellurate). The structural results including atomic positions, cation distributions, metal–oxygen distances and metal–oxygen–metal angles point to a progressive cation ordering on both sites of the Tb_7O_{12}-type structure with a strong preference of the smaller $4d^{10}$ cations (Sn^{4+}, Sb^{5+}, Te^{6+}) for the octahedral sites. The corresponding increase of the overall structure-bonding anisotropy is analyzed in terms of the crystal chemical properties of the OM_4 tetrahedral network of the antistructure. The relationships between the M_7O_{12} and the M_2O_3 bixbyite-type structures are explored. Within the whole series of compositions $In_{4+x}M_{3-x}O_{12}$ (M = Sn, Sb, Te) there exists an increase of the symmetry gap between the more symmetrical bixbyite structure and the M_7O_{12} type. This is tentatively correlated with the progressive weakening of thermal stability of these compositions from Sn to Te via Sb.

Keywords: Indium–tin antimonates; d^{10} cations ordering; Transparent conductors; Time of Flight Neutron Diffraction

1. Introduction

The recent synthesis of the transparent conductors $In_{4+x}Sn_{3-2x}Sb_xO_{12}$ with the Tb_7O_{12} fluorite-like structure [1], showed that the introduction of antimony in this solid solution enhances the electronic conductivity by one order of magnitude [2] with respect to $In_4Sn_3O_{12}$ [3], the optical transparency being unchanged. In this structure, the oxygen atoms and anionic vacancies are ordered, forming two sorts of sites with an octahedral and a sevenfold coordination, respectively, so that a cation ordering is favored (Fig. 1), as shown for example in the oxides Y_6UO_{12} [4], Lu_6UO_{12} [4] and In_6WO_{12} [5,6]. In the latter compounds the sevenfold sites are fully occupied by the trivalent cations (Y^{3+}, Lu^{3+}, In^{3+}), whereas the smaller cations (U^{6+}, W^{6+}) sit in the octahedral sites. In the case of $In_4Sn_3O_{12}$ [7], the octahedral 3(*a*) sites are fully occupied by Sn^{4+}, due to its smaller size and higher charge as In^{3+} cations and the rest of Sn^{4+} species are randomly distributed over the sevenfold 18(*f*) sites.

The X-ray Powder Diffraction (XRPD) of the solid solution $In_{4+x}Sn_{3-2x}Sb_xO_{12}$ [2] did not allow to determine the cationic distribution in this structure, due to the isoelectronic character of the $4d^{10}$ cations In^{3+}, Sn^{4+} and Sb^{5+}. For $x = 1.5$, it was just suggested that the Sb^{5+} cations are located in the octahedral sites in agreement with the smaller M–O distances observed for the latter.

In this paper, we present a Time of Flight Neutron Powder Diffraction (TOF NPD) study of four compositions of the solid solution $In_{4+x}Sn_{3-2x}Sb_xO_{12}$, including the limiting one $In_{5.5}Sb_{1.5}O_{12}$, in order to define simultaneously the cationic distribution, the distortion of the coordination polyhedra and the related anisotropy of the metal–oxygen bonding in comparison to the bixbyite structure. The field of comparison of the isoelectronic $4d^{10}$-type cations was enlarged to Te^{6+} which is involved in the existence of the mixed tellurate In_6TeO_{12} which is previously unreported.

*Corresponding author. Fax: +33 231 95 1600.
E-mail address: jacques.choisnet@ensicaen.fr (J. Choisnet).

0022-4596/$ - see front matter © 2007 Elsevier Inc. All rights reserved.
doi:10.1016/j.jssc.2006.12.031

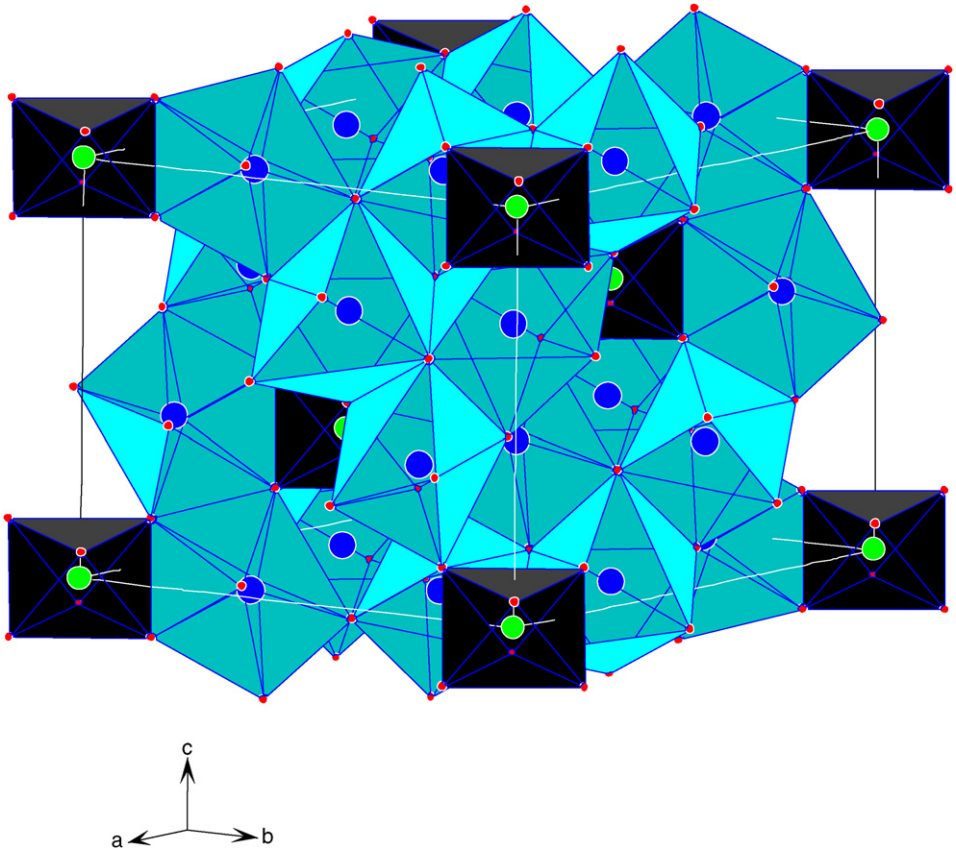

Fig. 1. Hexagonal cell of the fluorite-like oxygen-deficient M_7O_{12} structure. Black: (U^{6+}, W^{6+})O_6 octahedra and grey: sevenfold-coordinated (Y^{3+}, Lu^{3+}, In^{3+})O_7 polyhedra.

2. Experimental

A series of nine compositions of the solid solution $In_{4+x}Sn_{3-2x}Sb_xO_{12}$ ($x = 0.33$; 0.50; 0.66; 0.83; 1; 1.16; 1.33; 1.42; 1.5) was prepared from mixtures of pure In_2O_3, SnO_2 and Sb_2O_3, in alumina crucibles heated in air. As previously emphasized when preparing these phases for the first time [2], an initial heating at 600 °C is needed to ensure the full oxidation of Sb(III) into Sb(V). Then repeated annealings, followed by air quenching, were performed at increasing temperatures up to 1400 °C for the compositions whose antimony content is not larger than $x = 1$. For the values $1 < x \leqslant 1.5$, the final temperature did not exceed 1250 °C in order to prevent any decomposition. According to these experimental procedures, monophasic samples were obtained. Concerning In_6TeO_{12}, TeO_2 was used as precursor. The oxidation of Te(IV) to Te(VI) is even more difficult than that of Sb(III) to Sb(V). The starting mixture was heated in air for 3 days in the range 600–700 °C and then progressively, up to 1000 °C for 6 h. Under these conditions, a phase isotypic to the Sb-containing solid solution was isolated. From XRPD-phase analysis, In_6TeO_{12} is accompanied by some faint amount of In_2O_3 bixbyite. Any further heating at 1000 °C triggers a decomposition of In_6TeO_{12} into In_2O_3 and a volatilization of the tellurium oxide.

TOF powder neutron diffraction data were collected on the POLARIS high flux, medium-resolution diffractometer at the UK pulsed spallation neutron source ISIS, Rutherford Appleton Laboratories [8]. Four different compositions of the $In_{4+x}Sn_{3-2x}Sb_xO_{12}$ solid solution ($x = 0.50$; 0.66; 1 and 1.5) were loaded into a thin-walled vanadium can and data collected at room temperature.

The main purpose of the TOF study is to clear up the problem of the cationic distribution. Although it is not so large, the difference of the Fermi lengths of Sb(5.57) and Sn(6.22) is reasonably expected to allow a distinction of these elements; undoubtedly Sb and Sn will be not confused with In(4.07). As usual, a significant improvement of the location of the oxygen atoms will be of interest to match the calculated M–O distances with the theoretical one. Four compositions of the solid solution $In_{4+x}Sn_{3-2x}Sb_xO_{12}$ ($x = 0.50$; 0.66; 1; 1.5) were retained for a TOF structural analysis. The results of a previous neutron powder diffraction study was used for $x = 0$, i.e. $In_4Sn_3O_{12}$ [7]. Remaining compositions and the mixed tellurate In_6TeO_{12} as well, were considered for an XRPD structural analysis. In the Rietveld refinements the Fullprof program was used [9].

3. Results and discussion

3.1. TOF NPD calculations and cation ordering

The structural model of $In_4Sn_3O_{12}$ [7] was used: space group $R\bar{3}$. The hexagonal multiple cell includes two sets of cationic positions 3(*a*), 18(*f*) and two sets of oxygen positions 18(*f*). Results obtained from the Rietveld TOF NPD analysis of four compositions of the solid solution $In_{4+x}Sn_{3-2x}Sb_xO_{12}$ are reported in Table 1 in terms of atomic parameters including the occupancy of the cationic sites. For comparison, the data concerning $In_4Sn_3O_{12}$ ($x = 0$) [7] and our previous results obtained from XRPD Rietveld analysis for $In_{5.5}Sb_{1.5}O_{12}$ [2] are also reported. The values of the atomic parameters (positional coordinates and isotropic displacement parameters calculated from TOF NPD (compositions $x = 0.5$; 0.67; 1; 1.5) are very similar for each composition, they vary within the standard deviation. As compared to NPD results of $In_4Sn_3O_{12}$ [7], the variation of the atomic parameters of the oxygen atoms exceed their standard deviation, this being the likely consequence of the introduction of Sb^{5+} cations. The comparison of the TOF NPD and XRPD results for the same composition $x = 1.5$, i.e. $In_{5.5}Sb_{1.5}O_{12}$ brings a clear evidence for the improvement of the accuracy of the values of the atomic parameters of the oxygen atoms (the values obtained for the so-called heavy atoms are very close to each other). This is of importance for the interatomic distances, as discussed further. Fig. 2 shows an example of a typical fit after refining the composition $x = 0.5$. As it was decided to systematically include in the calculation procedure the two possible extra phases In_2O_3 and SnO_2 one can notice the presence of two series of corresponding supplementary bars. In the retained example $In_{4.5}Sn_2Sb_{0.5}O_{12}$ the calculated amount of the extra phases is equal to 3(1)%–In_2O_3– and 2(1)%–SnO_2–. Within the series of four compositions the maximum calculated amount of an extra phase does not exceed 5 wt% for In_2O_3 in $In_{5.5}Sb_{1.5}O_{12}$. Owing to the 10% difference between the Fermi lengths of Sb and Sn, which prevents to get accurate results when refining the phase composition, the nominal composition was systematically considered during the course of the calculation procedure.

Table 1
Atomic parameters of the compositions $In_{4+x}Sn_{3-2x}Sb_xO_{12}$ –SG $R\bar{3}$– from Rietveld analysis of TOF NPD data for $x = 0.5$–0.67–1–1.5 and for comparison, NPD data and XRPD data for $x = 0$ [7] and $x = 1.5$ [2], respectively

Composition Formula	$x = 0$ [7] $In_4Sn_3O_{12}$	$x = 0.5$ $In_{4.5}Sn_2Sb_{0.5}O_{12}$	$x = 0.67$ $In_{4.67}Sn_{1.67}Sb_{0.67}O_{12}$	$x = 1$ In_5SnSbO_{12}	$x = 1.5$ $In_{5.5}Sb_{1.5}O_{12}$	$x = 1.5$ [2] $In_{5.5}Sb_{1.5}O_{12}$
Hex. cell						
a_h (Å)	9.4634(2)	9.4535(1)	9.4530(1)	9.4479(1)	9.4547(1)	9.4545(1)
c_h (Å)	8.8556(2)	8.8815(1)	8.8891(1)	8.9035(1)	8.9219(1)	8.9210(2)
Cation 3(*a*)	0.54(6)	0.38(8)	0.34(12)	0.41(11)	0.25(7)	0.26(9)
B (Å^2)	Sn 100	Sn 75(6)	Sn 60(10)	Sn 42(8)	Sb 100	Sb 100
Occupancy %		Sb 25(6)	Sb 40(10)	Sb 58(8)		
Cation 18(*f*)						
x	0.2526(2)	0.2522(3)	0.2523(5)	0.2520(4)	0.2516(5)	0.2518(2)
y	0.2145(2)	0.2150(3)	0.2150(5)	0.2149(4)	0.2149(5)	0.2143(2)
z	0.3497(2)	0.3514(3)	0.3517(5)	0.3519(4)	0.3521(5)	0.3497(2)
B (Å^2)	0.47(4)	0.35(4)	0.34(7)	0.40(6)	0.41(5)	0.28(4)
Occupancy	In 67	In 75 Sn 21(1)	In 78 Sn 18(2)	In 83	In 92 Sb 8	In 92 Sb 8
%	Sn 33	Sb 4(1)	Sb 4(2)	Sn 10(1) Sb 7(1)		
Oxygen (1)						
18(*f*)	0.1979(2)	0.1938(3)	0.1928(5)	0.1907(4)	0.1893(4)	0.1920(17)
x	0.1768(2)	0.1704(3)	0.1690(5)	0.1664(4)	0.1645(4)	0.1653(27)
y	0.1162(2)	0.1172(3)	0.1173(5)	0.1171(4)	0.1173(4)	0.1073(15)
z	0.96(4)	0.87(5)	0.83(8)	0.84(7)	0.90(6)	2.4(5)
B (Å^2)						
Oxygen (2)						
18(*f*)	0.1886(3)	0.1918(4)	0.1924(5)	0.1938(4)	0.1947(5)	0.1921(23)
x	0.9745(2)	0.9753(4)	0.9754(5)	0.9759(4)	0.9759(5)	0.9775(23)
y	0.3917(2)	0.3934(3)	0.3937(4)	0.3945(4)	0.3949(4)	0.3830(14)
z	0.82(3)	0.70(4)	0.68(7)	0.63(6)	0.70(5)	1.8(4)
B (Å^2)						
*Rb%	4.4	^{1}3.1 ^{2}1.7 ^{3}2.9	^{1}3.2 ^{2}1.7 ^{3}2.7	^{1}2.6 ^{2}1.4 ^{3}3.1	^{1}4.1 ^{2}3.8 ^{3}5.0	8.2
*Rp%	—	^{1}8.6 ^{2}8.0 ^{3}7.8	^{1}9.7 ^{2}7.7 ^{3}7.8	^{1}7.5 ^{2}7.1 ^{3}7.1	^{1}10.5 ^{2}15.1 ^{3}12.4	17.5
*Rwp%	11.1	^{1}7.6 ^{2}6.8 ^{3}7.0	^{1}8.3 ^{2}6.6 ^{3}7.0	^{1}6.7 ^{2}6.2 ^{3}6.2	^{1}8.0 ^{2}8.9 ^{3}8.1	14.1

*Reliability factors are reported for the three banks of TOF data.

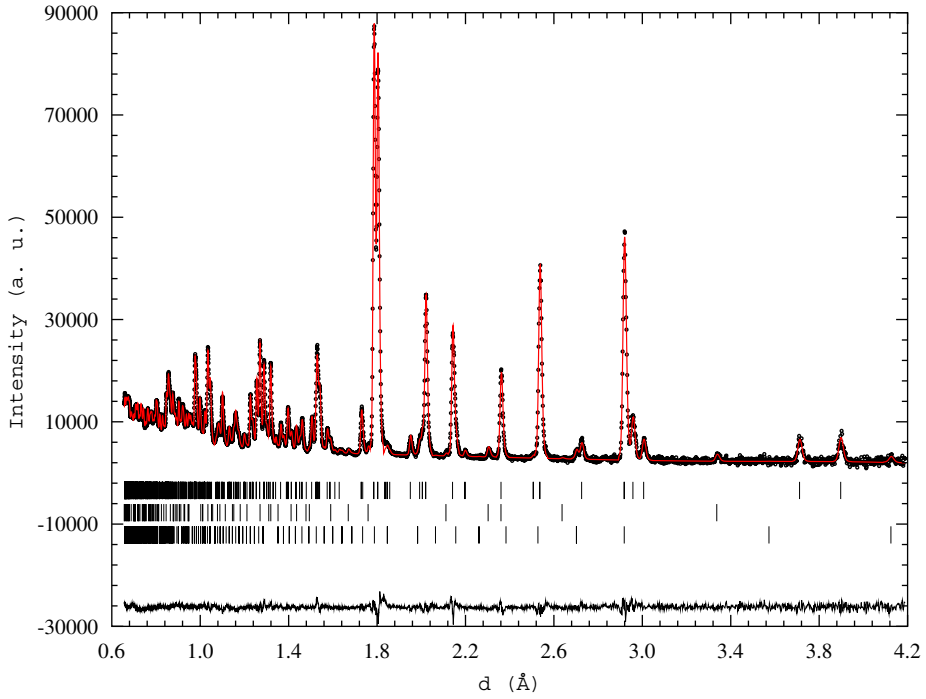

Fig. 2. Observed (dots) and calculated (lines) and difference TOF NPD profiles of $In_{4.5}Sn_2Sb_{0.5}O_{12}$. Vertical bars indicate the positions of the reflections of the title phase (upper), SnO_2 (middle) and In_2O_3 (lower).

Regarding the cationic distribution in the 3(*a*) and 18(*f*) sites, there is a significant variation depending on the extent of the double substitution $2\ Sn^{4+} \rightarrow In^{3+} + Sb^{5+}$. The obtained results demonstrate that Sn and Sb are simultaneously present over the two available sites, the octahedral 3(*a*) and the distorted sevenfold-coordinated 18(*f*). This is the main experimental result of this neutron diffraction study. At this stage, one important issue concerns the possible preferential occupancy of the octahedral 3(*a*) sites by Sb^{5+} due to its smaller size. Fig. 3 shows the refined Sb^{5+} occupancy in the 3(*a*) site versus the overall amount of Sb^{5+} and for comparison, the theoretical amount when considering a random distribution of the two cations Sb^{5+} and Sn^{4+}. Taking into account the calculated deviation of the cationic occupancy, one can state that the cationic distribution in the 3(*a*) sites is rather close to a random one with a very slight preference for Sb^{5+}.

To summarize, when going from the stannate $In_4Sn_3O_{12}$ to the antimonate $In_{5.5}Sb_{1.5}O_{12}$ there is an overall increase in cation ordering. The octahedral 3(*a*) sites are occupied by Sb^{5+} but there remains some partial disorder over the 18(*f*) sites due to the simultaneous presence of Sb^{5+}(8%) and In^{3+}(92%). As logically expected on the basis of its larger size, In^{3+} systematically orders with respect to both Sn^{4+} and Sb^{5+} and occupies the distorted sevenfold-coordinated sites. Sn^{4+} and Sb^{5+} compete for the occupancy of the octahedral sites and when their overall amount exceeds the limiting content of the octahedral sites, they both occupy the sevenfold-coordinated sites together with In^{3+}.

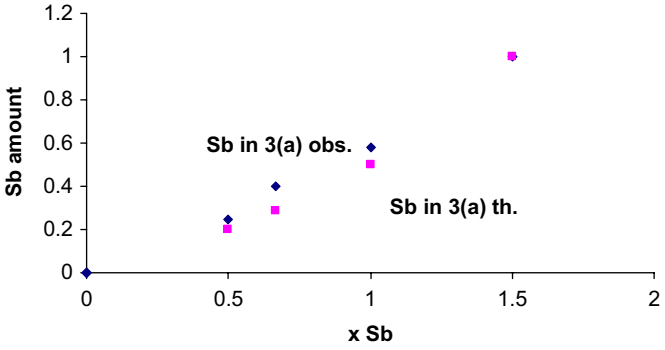

Fig. 3. Observed amount of Sb^{5+} sitting in the 3(*a*) sites in the solid solution $In_{4+x}Sn_{3-2x}Sb_xO_{12}$: observed values (upper) and theoretical values corresponding to a random distribution (lower).

3.2. Metal–oxygen distances and angular distortions: structure-bonding anisotropy

Table 2 reports the values of the metal–oxygen distances in five compositions ($x = 0$; 0.50; 0.67; 1; 1.50) of the solid solution. In order to enlarge the structural data of the M_7O_{12}-type oxides which contain $4d^{10}$ cations, the results obtained for the new tellurate In_6TeO_{12} are presented in Table 3, in terms of both atomic parameters (3*a*) and metal–oxygen distances (3*b*). As pointed out here above, In_6TeO_{12} cannot be prepared as a pure phase. The calculated amount of extra In_2O_3 is 13(1)%. In spite of their lower reliability, as usual when comparing the results of XRPD and NPD structural analysis, the metal–oxygen

Table 2
Metal-oxygen distances (Å) in the solid solution $In_{4+x}Sn_{3-2x}Sb_xO_{12}$ –SG $R\bar{3}$–

Composition	$x = 0$	$x = 0.5$	$x = 0.67$	$x = 1$	$x = 1.5$
Formula	$In_4Sn_3O_{12}$ [7]	$In_{4.5}Sn_2Sb_{0.5}O_{12}$	$In_{4.67}Sn_{1.67}Sb_{0.67}O_{12}$	In_5SnSbO_{12}	$In_{5.5}Sb_{1.5}O_{12}$
Hex. cell					
a_h (Å)	9.4634(2)	9.4535(1)	9.4530(1)	9.4479(1)	9.4547(1)
c_h (Å)	8.8556(2)	8.8815(1)	8.8891(1)	8.9035(1)	8.9219(1)
M–O_1 in $3(a) \times 6$	2.057(2)	2.021(3)	2.013(5)	1.992(4)	1.983(5)
M = Sn, Sb	Sn	$Sn_{0.75}Sb_{0.25}$	$Sn_{0.60}Sb_{0.40}$	$Sn_{0.42}Sb_{0.58}$	Sb
M–O in 18(f)					
M–$O_1 \times 1$	2.118(3)	2.141(4)	2.146(5)	2.158(4)	2.163(4)
M–$O_1 \times 1$	2.145(3)	2.191(4)	2.200(5)	2.218(4)	2.237(4)
M–$O_1 \times 1$	2.643(3)	2.658(4)	2.659(5)	2.666(4)	2.673(4)
M–$O_2 \times 1$	2.070(3)	2.075(4)	2.076(5)	2.077(4)	2.082(4)
M–$O_2 \times 1$	2.146(3)	2.127(4)	2.124(5)	2.118(4)	2.112(4)
M–$O_2 \times 1$	2.178(3)	2.190(4)	2.195(5)	2.200(4)	2.203(4)
M–$O_2 \times 1$	2.313(3)	2.286(4)	2.283(5)	2.274(4)	2.274(4)
Average	2.230	2.238	2.240	2.244	2.249
M = In, Sn, Sb	$In_{0.67}Sn_{0.33}$	$In_{0.75}Sn_{0.21}Sb_{0.04}$	$In_{0.78}Sn_{0.18}Sb_{0.04}$	$In_{0.83}Sn_{0.10}Sb_{0.07}$	$In_{0.92}Sb_{0.08}$

Table 3a
Atomic parameters of In_6TeO_{12} –SG $R\bar{3}$– from Rietveld analysis of XRPD data

Formula	In_6TeO_{12}
Hex. cell	
a_h (Å)	9.4407(2)
c_h (Å)	8.9943(3)
Te 3(a) B (Å^2)	0.19(7)
In 18(f)	
x	0.2507(3)
y	0.2144(2)
z	0.3545(2)
B (Å^2)	0.43(3)
Oxygen (1) 18(f)	
x	0.1825(18)
y	0.1520(28)
z	0.1178(17)
B (Å^2)	1.1(3)
Oxygen (2) 18(f)	
x	0.2000(24)
y	0.9823(24)
z	0.3925(17)
B (Å^2)	0.9(3)
*Rb%	3.8
*Rp%	10.2
*Rwp%	13.9

*Reliability factors are reported for the three banks of TOF data.

Table 3b
Metal–oxygen distances (Å) in In_6TeO_{12}

Formula	In_6TeO_{12}
Hex. cell	
a_h (Å)	9.4407(2)
c_h (Å)	8.9943(3)
Te–O_1 in $3(a) \times 6$	1.92(2)
In–O in 18(f)	
In–$O_1 \times 1$	2.22(3)
In–$O_1 \times 1$	2.33(3)
In–$O_1 \times 1$	2.68(3)
In–$O_2 \times 1$	2.02(3)
In–$O_2 \times 1$	2.24(3)
In–$O_2 \times 1$	2.11(3)
In–$O_2 \times 1$	2.29(3)
Average	2.27

distances observed in In_6TeO_{12} are considered in a tentative analysis of the overall series of $In_{4+x}M_{3-x}O_{12}$ phases with M = Sn, Sb, Te and $0 \leqslant x \leqslant 2$.

At first, the decrease of the $d3(a)$–O_1 distances in octahedral coordination versus x in the series of compositions $In_{4+x}M_{3-x}O_{12}$ (M = Sn, Sb, Te) (Fig. 4) corresponds well with the decrease of size: $r(Sn^{4+}) = 0.69$ Å → $r(Sb^{5+}) = 0.60$ Å → $r(Te^{6+}) = 0.56$ Å [10]. As compared

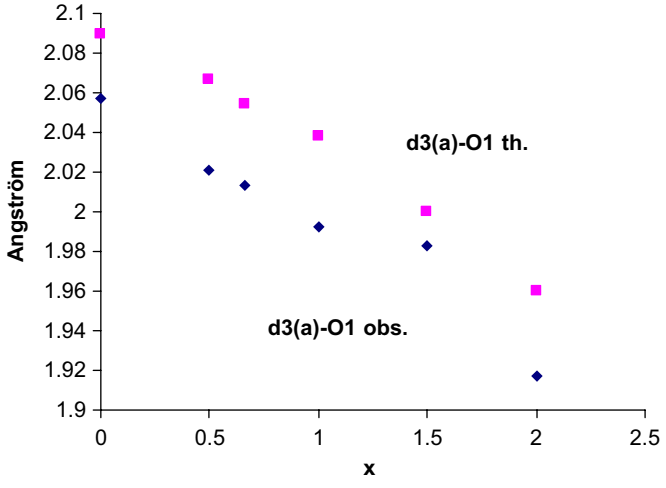

Fig. 4. Observed and theoretical values of the $d3(a)$–O_1 distances in the series $In_{4+x}M_{3-x}O_{12}$ (M = Sn, Sb, Te).

to the theoretical value calculated as the weighted sum of the M(Sn, Sb, Te)–O distances, the observed value of $d3(a)$–O_1 is systematically smaller by more than 0.03 Å, except in $In_{5.5}Sb_{1.5}O_{12}$ ($x = 1.5$) where the observed and theoretical values are nearly equal. We checked the valence sum rule at the 3(a) site (Fig. 5). In the Sb-containing compositions ($x = 0.5$; 0.67; 1; 1.5) the valence sum calculated on the basis of the site occupancy (Table 2) is somewhat larger than the atomic valence. As the valence-sum rule is fulfilled in $In_4Sn_3O_{12}$ ($x = 0$) and In_6TeO_{12} ($x = 2$), it can be reasonably assumed that there is a slight overbonding of the Sb^{5+} cations which sit in the 3(a) site. In connection with this result, an anomalous behavior of the cell constants in the antimony-rich compositions ($1 < x \leqslant 1.5$) will be discussed here after.

In the strongly distorted sevenfold coordination of the 18(f) sites the average value of d18(f)–O shows a very progressive slight increase with x, the amount of In^{3+} added to the site as shown in Fig. 6. Remarkably, this average value continuously fits the theoretical value calculated as the weighted sum of the M(In, Sn, Sb)–O distances. An analysis of the sevenfold coordination in terms of the two sets of oxygen atoms $O_{(1)}$ and $O_{(2)}$ (Fig. 6) brings evidence for a large difference of the corresponding d18(f)–O distances and consequently, the existence of a significant bonding anisotropy. As deduced from the large

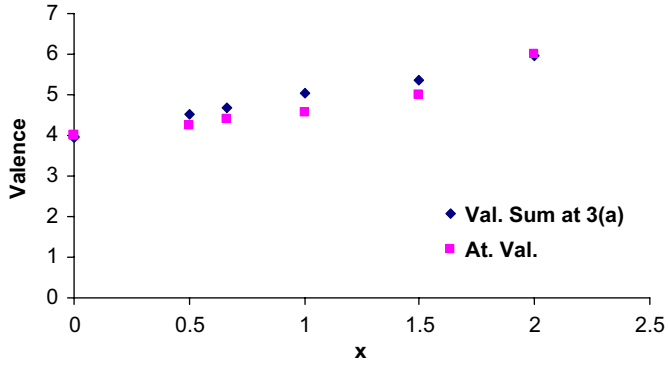

Fig. 5. Calculated valence-sum and atomic valence at the 3(a) site in the series $In_{4+x}M_{3-x}O_{12}$ (M = Sn, Sb, Te).

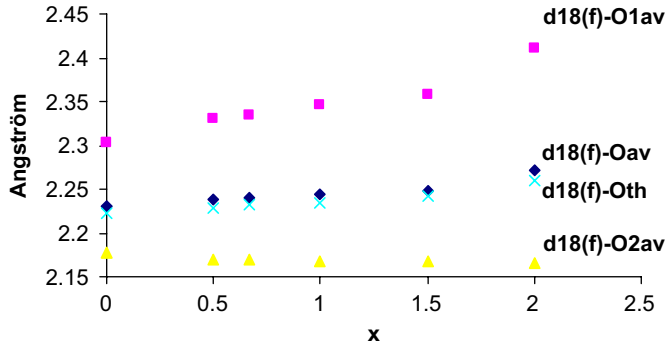

Fig. 6. Average and theoretical values of the d18(f)–O distances in the series $In_{4+x}M_{3-x}O_{12}$ (M = Sn, Sb, Te).

values of the d18(f)–$O_{(1)}$ distances, the underbonding of the 18(f) metals with the three O_1 atoms increases from $x = 0$ up to 2, i.e. when the site is fully occupied by In^{3+}. This underbonding is balanced by an overbonding between the 18(f) sites and the four $O_{(2)}$ atoms, since the d18(f)–$O_{(2)}$ distances are smaller than the average (Fig. 6). Furthermore, this overbonding seems to be rather constant within the whole extent of the series of compositions $In_{4+x}M_{3-x}O_{12}$.

A further insight into the oxygen bonding is of interest. As deriving from the fluorite model, the M_7O_{12} structure can be analyzed in terms of a tetrahedral antistructure. There exists a face-centered cubic network of cations (..*ABC*.. compact sequence), where 6/7 of the tetrahedral sites are filled by oxygen atoms. The existence of an ordering on both the metallic and oxygen networks, 1/6 and 1/1, respectively, results in the following topological property: each $O_{(1)}$ oxygen atom is tetrahedrally bonded to one 3(a) cation (Sn^{4+}, Sb^{5+}, Te^{6+}) and three 18(f) cations, whereas each $O_{(2)}$ oxygen atom is bonded to four 18(f) cations. In this way, the structure-bonding anisotropy of the M_7O_{12} structure can be well understood:

- one-half of the OM_4 tetrahedra, namely the $O_{(1)}M_4$ one is strongly distorted, as visible from both the O–M distances deviations and the M–O–M angular deviations (Fig. 7), the deviations being defined as the difference between the largest and the smallest values of an O–M distance and a M–O–M angle, respectively. These deviations regularly increase with x in the compositions $In_{4+x}M_{3-x}O_{12}$. The highest deviation is observed in In_6TeO_{12} in agreement with the bonding of $O_{(1)}$ with both In^{3+} and Te^{6+} whose size difference is the largest: $\Delta r = 0.24$ Å;
- the other half of the OM_4 tetrahedra, the $O_{(2)}M_4$ one, behaves in a very different way. The distance deviation (Fig. 7) is more than two times smaller than in the $O_{(1)}M_4$ tetrahedra and it decreases as x increases up to $x = 1.5$. Note that $dO_{(2)}$–M_4 increases when x reaches the value 2, but this increase must be considered cautiously due to the rather poor reliability of the atomic coordinates of the oxygen atoms which are calculated in In_6TeO_{12}. The angular deviation (Fig. 7) slightly decreases as x increases up to $x = 2$. In the latter case, i.e. In_6TeO_{12} the angular deviation is significantly smaller in the $O_{(2)}M_4$ tetrahedra than in the $O_{(1)}M_4$ one by at least 10°.

At this stage it is necessary to emphasize that the structure-bonding anisotropy of the M_7O_{12} structure is connected with the cation ordering phenomena in a rather simple way. The more the cationic network is ordered, the more the overall structure-bonding anisotropy increases. More precisely, two properties are very likely to occur:

- the distribution of the oxygen bonding in the $O_{(2)}M_4$ tetrahedra (M only in 18(f) sites) is less anisotropic than

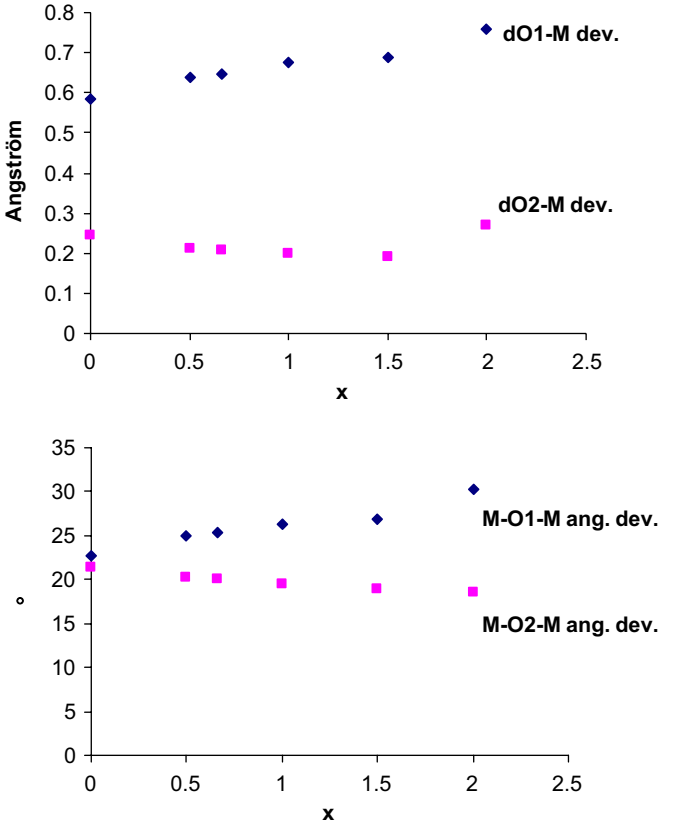

Fig. 7. From top to bottom: distances deviations and angular deviations in the $O_{(1)}M_4$ and $O_{(2)}M_4$ tetrahedra of the series $In_{4+x}M_{3-x}O_{12}$ (M = Sn, Sb, Te).

the distribution of the oxygen bonding in the $O_{(1)}M_4$ tetrahedra (M in both 18(f) and 3(a) sites).

- the progressive increase of the cation ordering on both sites has no significant effect on the anisotropy of the $O_{(2)}$ oxygen bonding, whereas it triggers a further increase of the anisotropy of the $O_{(1)}$ oxygen bonding.

3.3. Relationships between the M_7O_{12} structure of the compositions $In_{4+x}M_{3-x}O_{12}$ (M = Sn, Sb, Te) and the M_2O_3 bixbyite

During the course of the synthesis of the series of compositions $In_{4+x}M_{3-x}O_{12}$ (M = Sn, Sb, Te,) it was observed that the antimony-rich compositions ($1<x\leqslant 1.5$) and above all the tellurate In_6TeO_{12} are metastable phases at high temperature. As herein pointed out, above 1250 °C or 1000 °C, respectively, the bixbyite phase In_2O_3 is more stable than the M_7O_{12} phase. In order to understand the occurrence of this "transformation", it was decided to look into the relationships between the M_7O_{12} and M_2O_3 bixbyite structures.

First of all, the variation of the constants of the hexagonal multiple cell of the compositions $In_{4+x}M_{3-x}O_{12}$ was considered. Fig. 8 shows the dependence of the cell volume, a_h and c_h the cell parameters, on x the amount of added In^{3+}. The overall cell volume increases with two well-defined regimes from both sides of the composition $x=1$: there is a weaker slope for $x\leqslant 1$ and a larger one for $x>1$. The variation of a_h and c_h is rather surprising: a_h and c_h show a fully different dependence on x, a decrease and an increase, respectively, which both show an overall linearity between the limiting compositions $x=0$ and 2. In the intermediate range of compositions $1<x\leqslant 1.5$, i.e. the antimony-rich one, there exists an anomalous dependence of the cell constants: a_h decreases for $0<x<1$ and then increases, whereas c_h increases over the whole compositional range.

A better understanding of the rather unusual properties of the cell constants, namely the singularity of the composition $x=1$, was assumed to be found in the relationships between the M_7O_{12} and M_2O_3 bixbyite structures which both derive from the fluorite model of the MO_2 oxides (fluorite-like formula $MO1.71$ and $MO1.5$, respectively). More precisely, a_{Rh} the parameter of the rhombohedral cell, as related to a_h and c_h the parameters of the hexagonal cell, is expected to reveal a cooperative effect of the geometrical components along a_h and c_h. Furthermore, a_{Rh} features the shortest distance between the M metals (M = Sn, Sb, Te) which occupy the 1(a) positions (0, 0, 0) in the rhombohedral unit cell. Fig. 9 shows the variation of a_R in the whole series of compositions

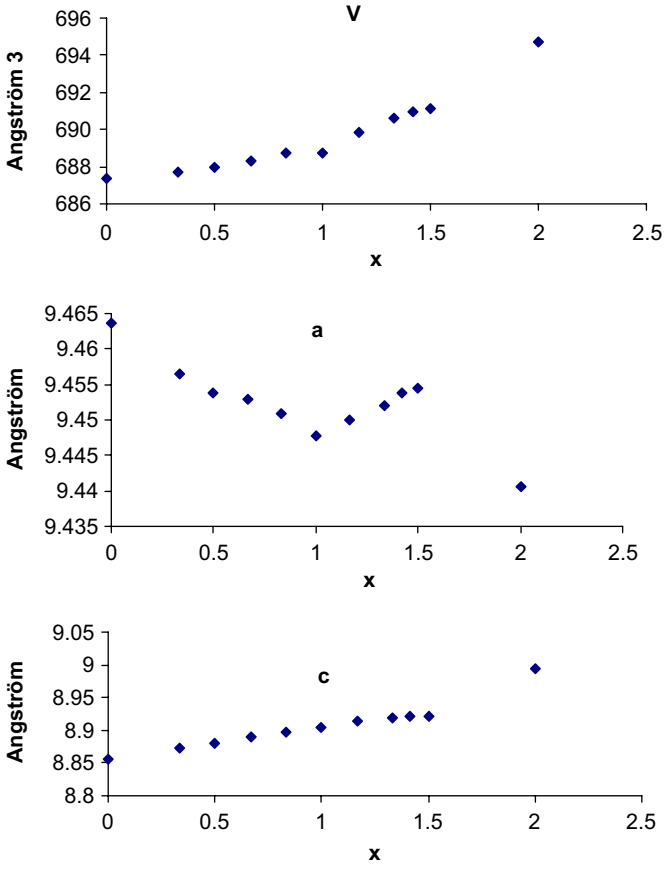

Fig. 8. Variation of the constants of the hexagonal multiple cell in the series $In_{4+x}M_{3-x}O_{12}$ (M = Sn, Sb, Te). From top to bottom: V volume, a_h and c_h.

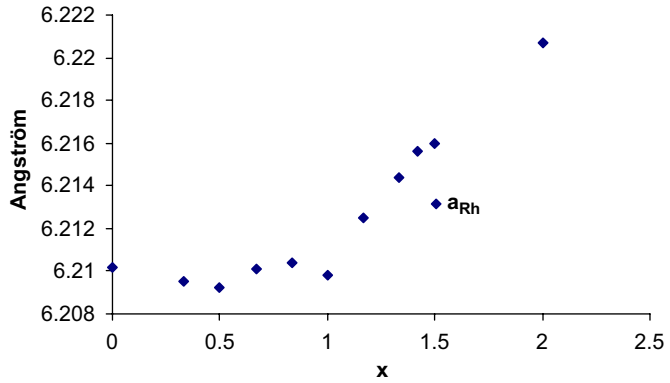

Fig. 9. Variation of a_{Rh} parameter of the rhombohedral unit cell in the series $In_{4+x}M_{3-x}O_{12}$ (M = Sn, Sb, Te).

$In_{4+x}M_{3-x}O_{12}$. Clearly, the composition $x = 1$ separates two fully different regimes. Up to $x = 1$, i.e. the composition In_5SnSbO_{12}, the value of a_{Rh} is nearly constant and equal to 6.21 Å, whereas for the values of x larger than 1 and up to $x = 2$ a linear increase occurs. This means that the shortest M–M (M = Sn, Sb) distance, from $In_4Sn_3O_{12}$ to In_5SnSbO_{12}, is unsensitive to the indium enrichment of 6/7 of the cations which triggers an increase of the average cationic size. Then for $x > 1$ a cooperative effect takes place and the M–M distances have a concern with the overall expansion of the cell. The metastability of the M_7O_{12} structure of the series of compositions $In_{4+x}M_{3-x}O_{12}$, which transforms to the bixbyite type for $x > 1$ is likely to be connected to this phenomenon.

4. Concluding remarks

The results of the structural study of the solid solution $In_{4+x}Sn_{3-2x}Sb_xO_{12}$ and In_6TeO_{12} offer relevant information regarding the crystal chemistry of their M_7O_{12} fluorite-like ordered structure and this, in comparison to the bixbyite structure. Furthermore, there is a unique opportunity to bring together the entire series of $4d^{10}$-type cations—In^{3+}, Sn^{4+}, Sb^{5+}, Te^{6+}—which has a big concern with the solid-state chemistry of complex oxides. The combined effects of a strong decrease of the cationic radius from 0.80 to 0.56 Å in octahedral coordination and a significant increase of the covalency of the metal–oxygen bonding from In to Te result in a main trend: there is an increasing ordering of the cations from $In_4Sn_3O_{12}$ to In_6TeO_{12}, more precisely from a moderately ordered phase to a perfectly fully ordered one, via a competition between Sn^{4+} and Sb^{5+} which practically do not order with respect to each other. Simultaneously, the metal–oxygen bonding shows an increasing anisotropy between the two sets of oxygen atoms $O_{(1)}$ and $O_{(2)}$.

The symmetry gap between the both more ordered and more distorted M_7O_{12} structure and the bixbyite increases within the whole series of compositions $In_{4+x}M_{3-x}O_{12}$ (M = Sn, Sb, Te), i.e. it is the smallest in $In_4Sn_3O_{12}$ and the largest in In_6TeO_{12}. The likely reason has to be found in the highly anisotropic distribution of the cationic radii, as the average cationic size of 6/7 of the cations increases whereas it decreases for the remaining seventh. Accordingly, $In_4Sn_3O_{12}$ is a stable phase up to temperatures larger than 1500 °C whereas In_6TeO_{12} undergoes the decomposition at 1000 °C. An intermediate behavior occurs in the solid solution $In_{4+x}Sn_{3-2x}Sb_xO_{12}$ whose thermal stability of compositions $x > 1$ vanishes at temperatures exceeding 1250 °C. In fact, in the intermediate range of compositions ($1 < x \leqslant 1.5$), the antimony-rich one, a significant trend to reduce the symmetry gap between the M_7O_{12} and M_2O_3 bixbyite structures takes place. One can tentatively assume that this phenomenon is connected with a partial disorder of the cationic distribution on both sites, three cations and two cations over 6/7 and one-seventh of the cationic sites, respectively.

At last and probably of great importance, one has to consider the potential role of the cation ordering and above all the case of Sn^{4+} and Sb^{5+} on the conductivity of these materials. A preliminary study of the electronic band structure of In_5SnSbO_{12} as compared to $In_4Sn_3O_{12}$ was based on the structural results of a XRPD Rietveld procedure, assuming that the octahedral 3(*a*) sites are fully occupied by Sb^{5+} [11]. It was found that there is a further splitting of the conduction band with respect to $In_4Sn_3O_{12}$, which changes the dispersion of the conduction band of In_5SnSbO_{12} and could be the driving force of the observed enhancement of the electrical conductivity, namely one order of magnitude with respect to $In_4Sn_3O_{12}$. In fact, the actual TOF NPD structure refinements demonstrate the simultaneous presence of both Sn^{4+} and Sb^{5+} in the 3(*a*) sites and the 18(*f*) one with a nearly random distribution. At the moment it is not possible to evaluate the consequence of this new data. One can only assume drastic changes in the calculation of the band structure not to occur. Very likely it will be found, as previously, that the top of the valence band is mainly formed by O 2*p* states with some In 5*d* character, whereas the bottom of the conduction band is due primarily to the Sn 5*s* electrons at the 18(*f*) sites. Work is in progress to elucidate this problem.

Acknowledgments

This work was performed in the frame of the European Network of Excellence FAME. One of us—L.B.—is grateful to the Commission of European Communities for receiving a Marie Curie Action: Contract MEST-CT-2004 6 514237 with a specific Host Fellowship for Early Stage Researchers Training.

References

[1] J. Zhang, R.B. Von Dreele, L. Eyring, J. Solid State Chem. 104 (1993) 21.
[2] J. Choisnet, L. Bizo, R. Retoux, S. Hébert, B. Raveau, J. Solid State Chem. 177 (2004) 3748.

[3] T. Minami, Y. Takeda, S. Takata, T. Kakumumi, Thin Solid Films 308 (1997) 13.
[4] S. Bartram, Inorg. Chem. 5 (1966) 749.
[5] D. Michel, A. Kahn, Acta Crystallogr. B 38 (1982) 1437.
[6] A.P. Richard, D.D. Edwards, J. Solid State Chem. 177 (2004) 2740.
[7] N. Nadaud, N. Lequeux, M. Nanot, J. Jové, T. Roisnel, J. Solid State Chem. 135 (1998) 140.
[8] R.I. Smith, S. Hull, User guide for the Polaris Powder Diffractometer at ISIS, CCLRC Technical Report, RAL-TR-97-038, 1997.
[9] J. Rodriguez-Carvajal, Program Fullprof, 1997, p. 5
[10] R.D. Shannon, C.T. Prewitt, Acta Crystallogr. B 25 (1969) 925.
[11] C.Y. Ren, S.H. Chiou, J. Choisnet, J. Appl. Phys. 99 (2006) 23706.